Electronic Supplementary Material (ESI) for CrystEngComm.

Remarkable decrease in stiffness of aspirin crystals upon reducing crystal size to nanoscale dimensions via sonochemistry

Kristin M. Hutchins, Thilini P. Rupasinghe, Shalisa M. Oburn, Kamal K. Ray, Alexei V. Tivanski,* and Leonard R. MacGillivray*

Department of Chemistry, University of Iowa, Iowa City, Iowa 52242-1294, USA
Author email addresses: alexei-tivanski@uiowa.edu; len-macgillivray@uiowa.edu

Supplementary Information:

1) Synthesis of macro- and nano-sized crystals

Materials: Acetylsalicylic acid (aspirin) was purchased from Acros Organics and used without further purification.

Crystallizations: Macro-sized crystals of aspirin were grown *via* slow solvent evaporation in a concentrated solution of acetone.[1] Nano-sized crystals of aspirin were obtained *via* sonochemistry. Aspirin (200 mg, 1.1 mmol) was dissolved in 1 mL of acetone. The solution was rapidly injected directly into 175 mL of cold hexanes while exposed to low-intensity ultrasonic radiation (ultrasonic cleaning bath Branson 2510R-DTM, frequency: 42 kHz, 6% at 100 W). The resulting suspension was sonicated for 1-2 min, filtered, dried at room temperature, and analyzed *via* powder X-ray diffraction.

2) Single-crystal X-ray diffraction indexing

Single-crystal indexing was performed using a Nonius Kappa CCD single-crystal X-ray diffractometer at room temperature using Mo Kα radiation (λ = 0.71073 Å).

3) Powder X-ray diffraction measurements (PXRD)

PXRD data were obtained on a Siemens D5000 X-ray diffractometer using Cu $K\alpha_1$ radiation (λ= 1.54056 Å) (scan type: locked coupled; scan mode: continuous; step size: 0.02º; scan time: 2s/step). The samples were mounted on glass slides.

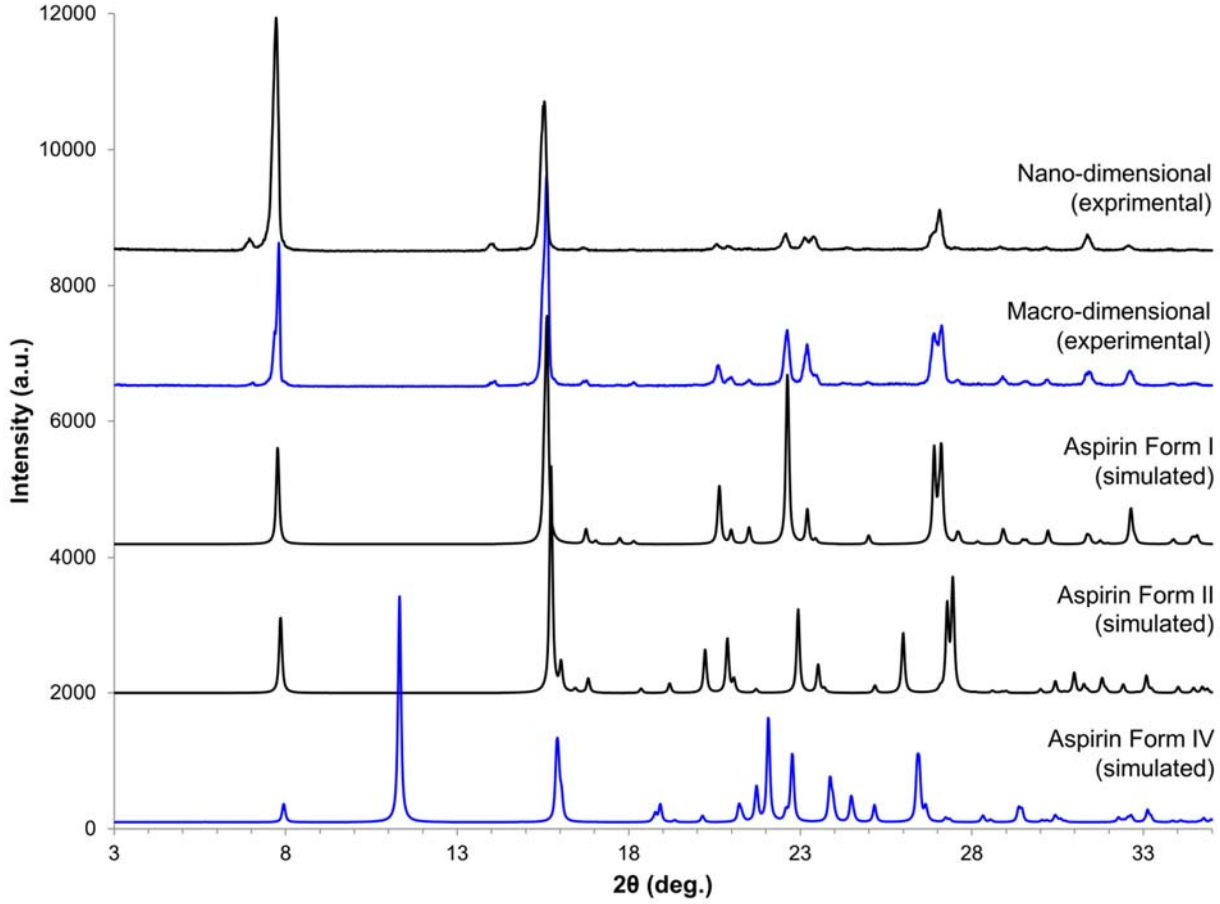

Figure S1. Comparison of aspirin PXRDs: simulated pattern from X-ray crystal data, macro-sized, and nano-sized.[2]

4) Scherrer equation calculations

The size of the nanocrystals from the bulk powder was calculated using the broadening in the PXRD peaks. The Scherrer equation (Eq S1) was used for the calculation:

$$L = \frac{K\lambda}{\beta\cos\theta} \qquad \textbf{Eq. S1}$$

where L is the mean size of the crystallites, K is the shape factor, λ is the X-ray wavelength, β is the line broadening at half of the maximum intensity in radians (after subtracting the instrumental line broadening), and θ is the angle.[3]

A shape factor of 0.9,[4] wavelength of 0.15406 nm (CuKα1), and the peak at 32.6° (2θ) (see Fig. S2) were used for the calculation. The β value for the peak is equal to 0.23307° and the instrumental line broadening was 0.05°. The calculation yielded a crystallite size of 51.5 nm.

5) Dynamic Light Scattering Measurements

DLS measurements were performed for the nano-dimensional aspirin crystals obtained through sonochemistry by dispersing the crystals in tetradecane. The mean size obtained for the nanocrystals is noted below. Measurement were made using a Zetasizer Nano ZS (Malvern Instruments).

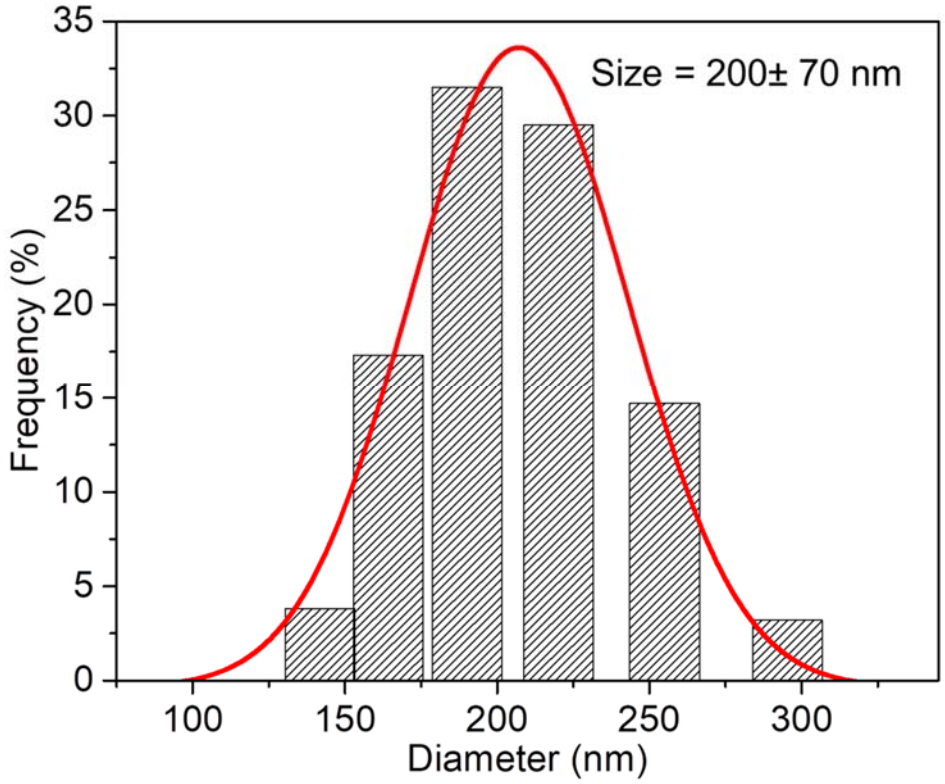

Figure S2. Gaussian distribution of nano-dimensional aspirin crystal sizes.

6) AFM imaging and nanoindentation measurements

Millimeter-sized crystals were directly placed on a freshly cleaved mica substrate and measurements were conducted using a closed Fluid cell (Fluid cell lite, Asylum Research, Santa Barbara, CA). Nano-sized crystalline samples were suspended in hexanes at 1.0 mg/mL and then deposited on a freshly cleaved atomically flat mica substrate (V-I grade, SPI Supplies, Westchester, PA). All AFM studies were conducted using a Molecular Force Probe 3D AFM (Asylum Research, Santa Barbara, CA). AFM height images and nanoindentation measurements were collected at room temperature using silicon probes (Mikromasch, San Jose, CA, CSC37) with a nominal spring constant of 0.35 N/m and a typical tip radius of curvature of 10 nm. The tip radius of curvature was verified using scanning electron microscopy and was found to be approximately 10 nm, as expected. Actual spring constants were determined using built-in thermal noise method.[5] Topographic images were collected using intermittent contact mode (AC mode) or contact mode at a typical scan rate of 1 Hz.

Force-displacement curves were recorded at 1 Hz in an organic solvent (olefin free n-tetradecane) that served to minimize the adhesion force between the probe and the surface. Each force-displacement curve was collected during AFM probe motion towards and away from the sample. Typical force plot involved the probe-started motion toward the sample from the height of approximately 200 nm above the surface that continued until the predetermined force of 10 nN was reached. Then the motion was reversed bringing the probe to approximately the initial height above the surface. The maximum force of 10 nN was used as no sign of mechanical damage on a crystal surface was observed under such conditions after a series of repeated force-displacement measurements.

To ensure the reproducibility of the measurements, typically 10-15 repeated force measurements were collected at each crystal location of nano-sized samples and at ~10 different locations on the each face of the millimeter-sized crystals. In addition, force plots were collected on the substrate approximately 100-150 nm away from the corresponding crystal position. Measurements on the substrate were used to calibrate the deflection sensitivity of the AFM cantilever to convert the force-displacement curve to force *versus* indentation depth plot.[6] Overall, 3 different AFM probes were used for the nanoindentation measurements.

The force *versus* indentation depth data were used to determine the Young's modulus of a crystal by fitting the approach data to the Hertzian contact model, which assumes purely elastic contact.[6-9] Since practically all force-displacement plots showed no deviation between the approach and retract data, the indentation can be assumed elastic thus facilitating the use of the model. The substrate-induced effects on the measured Young's modulus values were negligible under our experimental conditions since a typical height of a nanocrystal (ranging from 25 to 200 nm) is more than one order of magnitude larger than typical indentation depth of 1-3 nm.

As the Hertzian model assumes purely elastic contact without adhesion interactions, force curves with the adhesion force between the tip and crystal that was greater than 0.5 nN were not used in the data analysis. Additionally, force plots were also not considered when variation was observed between the approaches and retract data because such deviation represents inelastic effects.[6, 8c] Both criteria resulted in a removal of few percent of the total number of individual force indentation measurements used in the analysis. Representative loading force – indentation depth plots and Hertzian model fits for macro- and nano-sized aspirin crystals are shown in Figure S3. The Poisson's ratios of the Si_3N_4 AFM tip and aspirin nano- and macro-sized crystals were assumed to be 0.25 and 0.3, respectively.[7e,7f]

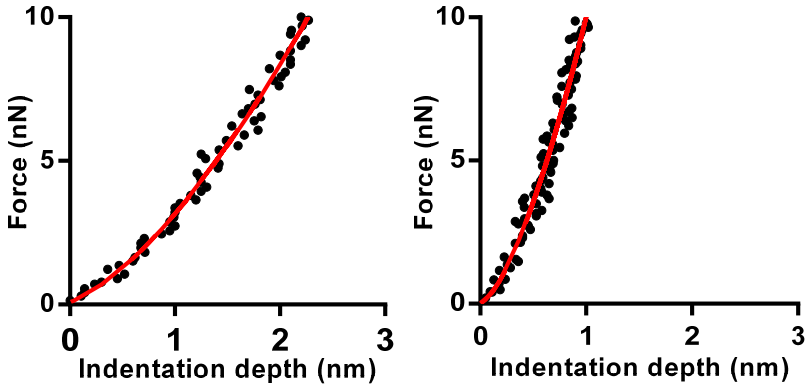

Figure S3. Representative force *versus* indentation depth data for nano-sized (left) and macro-sized (100) plane (right) aspirin (form I) crystals. Black dots are approach to the crystal surface data and red solid line is the fit to the Hertzian contact model used to calculate the corresponding Young's modulus value (here 520 MPa and 2.5 GPa for nano- and macro-sized crystals, respectively).

7) References

1. Y. Kim, K. Machida, T. Taga and K. Osaki, *Chem. Pharm. Bull.*, 1985, **33**, 2641.
2. Aspirin: (a) Form I: Y. Kim, K. Machida, T. Taga, K. Osaki, *Chem. Pharm. Bull.* 1985, **33**, 2641; Form II: A. D. Bond, R. Boese, G. R. Desiraju, *Angew. Chem., Int. Ed.* 2007, **46**, 618; (c) Form IV: A. G. Shtukenberg, C. T. Hu, Q. Zhu, M. U. Schmidt, W. Xu, M.T and, B. Kahr, *Cryst. Growth Des.* 2017, **17** , 3562.
3. A. L. Patterson, *Phys. Rev.*, 1939, **56**, 978.
4. A. Monshi, M. R. Foroughi and M. R. Monshi, *WJNSE*, 2012, **2**, 154.
5. J. L. Hutter and J. Bechhoefer, *Rev. Sci. Instrum.*, 1993, **64**, 1868.
6. S. Guo and B. B. Akhremitchev, *Langmuir*, 2007, **24**, 880.
7. (a) S. Guo and B. B. Akhremitchev, *Langmuir*, 2008, **24**, 880; (b) J.-G. Guo and Y.-P. Zhao, *J. Appl. Phys.*, 2005, **98**, 074306/1; (c) H. Hertz, *J. reine angew. Math*, 1881, **92**, 110; (d) L. R. Ditzler, C. Karunatilaka, V. R. Donuru, H. Y. Liu and A. V. Tivanski, *J. Phys. Chem. C*, 2010, **114**, 4429; (e) T. P. Rupasinghe, K. M. Hutchins, B. S. Bandaranayake, S. Ghorai, C. Karunatilake, D. K. Bučar, D. C. Swenson, M. A. Arnold, L. R. MacGillivray and A. V. Tivanski, *J. Am. Chem. Soc.* 2015, **137,** 12768; (f) H. Mohapatra, T. M. Kruger, T. I. Lansakara, A. V. Tivanski and L. L. Stevens, *Soft Matter,* 2017, **13**, 5684.
8. (a) N. J. Tao, S. M. Lindsay and S. Lees, *Biophys. J.*, 1992, **63**, 1165; (b) E. A-Hassan, W. F. Heinz, M. D. Antonik, N. P. D'Costa, S. Nageswaran, C.-A. Schoenenberger and J. H. Hoh, *Biophys. J* . 1998, **74**, 1564; (c) S. Guo and B. B. Akhremitchev, *Biomacromolecules*, 2006, **7**, 1630; (d) C. Karunatilaka, D.-K. Bučar, L. R. Ditzler, T. Friščić, D. C. Swenson, L. R. MacGillivray and A. V. Tivanski, *Angew. Chem. Int. Ed.*, 2011, **50**, 8642.
9. K. L. Johnson, *Contact Mechanics*, Cambridge University Press, Cambridge, U.K., 1985.